Hydrothermal Syntheses and Structural Characterization of Layered Oxovanadium Phosphate Solids Incorporating Organic Cations: $[H_2N(C_4H_8)NH_2][(VO)_4(OH)_4(PO_4)_2]$, $[(NH_3C_3H_6)NH(C_2H_4)_2NH(C_3H_6NH_3)][(VO)_5(OH)_2(PO_4)_4]\cdot 2H_2O$, $[HN(C_2H_4)_3NH]_2[(VO)_8(HPO_4)_3(PO_4)_4(OH)_2]\cdot 2H_2O$, and $[HN(C_2H_4)_3NH][(VO)_3(OH)_2(PO_4)_2]$

Victoria Soghomonian,[†] Qin Chen,[†] Yiping Zhang,[‡] Robert C. Haushalter,*[,‡] Charles J. O'Connor,[§] Cuihong Tao,[§] and Jon Zubieta*[,†]

Department of Chemistry, Syracuse University, Syracuse, New York 13244, NEC Research Institute, Princeton, New Jersey 08540, and Department of Chemistry, University of New Orleans, New Orleans, Louisiana 70148

Received December 7, 1994[⊗]

Four new two-dimensional vanadium phosphates, $[H_2N(C_4H_8)NH_2][(VO)_4(OH)_4(PO_4)_2]$ (**1**), $[(NH_3C_3H_6)NH(C_2H_4)_2NH(C_3H_6NH_3)][(VO)_5(OH)_2(PO_4)_4]\cdot 2H_2O$ (**2**), $[HN(C_2H_4)_3NH]_2[(VO)_8(HPO_4)_3(PO_4)_4(OH)_2]\cdot 2H_2O$ (**3**), and $[HN(C_2H_4)_3NH][(VO)_3(OH)_2(PO_4)_2]$ (**4**), have been synthesized by exploiting the hydrothermal technique. Compound **1** was synthesized from the reaction of a mixture VCl_4, H_3PO_4, piperazine, tetrabutylammonium hydroxide, and H_2O in the mole ratio 1:2.2:1.7:1.2:2830 heated at 200 °C for 48 h. Phosphate **2** was obtained from the reaction of VCl_4, H_3PO_4, 1,4-bis(aminopropyl)piperazine, and water in the mole ratio 1:2.4:6.3:1207 heated for 114 h at 150 °C. Compounds **3** and **4** were synthesized from the same reactants, VCl_4, H_3PO_4, 1,4-diazabicyclo[2.2.2]octane (DABCO), and H_2O under different reaction conditions. While the preparation of **3** employed the mole ratio 1:8.0:4.0:1375 and a heating time of 72 h at 200 °C, the synthesis of **4** required a ratio of 1:6.0:4.0:2268 at 200 °C for 48 h. While these four materials share a common motif of inorganic V/P/O layers separated by organic cations, each exhibits highly distinctive structural features. Phosphate **1** has discrete binuclear $\{V_2O_8\}$ edge-sharing units, which give rise to undulations in the inorganic V/P/O layer; while compound **2** possesses similar $\{V_2O_8\}$ units, the distinctive features of isolated VO_5 square pyramids and $\{V_2O_4P_2\}$ intersecting rings are also present. While compounds **3** and **4** have the same template, 1,4-diazabicyclo[2.2.2]octane, examination of the inorganic layers reveals different structural motifs. Compound **3** possesses two isolated tetrameric units: one composed of two face-sharing VO_6 octahedra, each sharing a corner with a $\{VO_5\}$ square pyramid, while the second consists of two pairs of corner-sharing $\{VO_5\}$ square pyramids, linked by μ_4-phosphate groups. In contrast, compound **4** contains binuclear units constructed from face-sharing $\{VO_6\}$ dimers linked by corner-sharing interactions into infinite chains. In addition each binuclear unit of **4** exhibits a corner-sharing interaction with a $\{VO_5\}$ square pyramidal site to produce a ribbon of octahedral−square pyramidal vanadium polyhedra; adjacent ribbons are linked through μ_4-phosphate groups. Crystal data are as follows. $C_4H_{16}N_2O_{16}P_4V_4$ (**1**): blue plates, monoclinic space group $P2_1/c$ (No. 14) with $a = 10.682(2)$ Å, $b = 8.991(2)$ Å, $c = 8.951(2)$ Å, $\beta = 110.41(3)°$, $V = 805.7(4)$ Å^3, $Z = 1$; refinement based on 1493 reflections gave a final residual of $R = 0.0569$. $C_{10}H_{34}N_4O_{25}P_4V_5$ (**2**): blue plates, triclinic space group $P\bar{1}$ (No. 2) with $a = 9.433(3)$ Å, $b = 17.799(3)$ Å, $c = 9.356(1)$ Å, $\alpha = 103.83(1)°$, $\beta = 91.80(2)°$, $\gamma = 95.90(2)°$, $V = 1514.7(6)$ Å^3, $Z = 2$; 3935 reflections, $R = 0.052$. $C_{12}H_{37}N_2O_{40}P_7V_8$ (**3**): blue plates, monoclinic space group $P2/n$ (No. 13) with $a = 9.559(2)$ Å, $b = 8.840(2)$ Å, $c = 24.309(5)$ Å, $\beta = 100.07(2)°$, $V = 2022.5(7)$ Å^3, $Z = 2$; 3181 reflections, $R = 0.0561$. $C_6H_{16}N_2O_{13}P_2V_3$ (**4**): ink-blue square plates, monoclinic space group $P2_1/n$ (No. 14) with $a = 12.048(2)$ Å, $b = 6.3470(10)$ Å, $c = 20249(4)$ Å, $V = 1493.5(8)$ Å^3, $Z = 4$; 1846 reflections, $R = 0.0567$.

Introduction

The contemporary interest in oxovanadium phosphate solid materials reflects not only their practical applications as catalysts[1] and inorganic ion exchangers[2] and their versatile intercalation properties but also their fundamental chemistry which is characterized by unusual structural complexity, encompassing a wide compositional range of both three-dimensional framework and two-dimensional network structures, and a concomitant diversity of electronic and magnetic properties.[3] Vanadyl phosphates, $[VOPO_4]$[4] and α-$[VOPO_4]\cdot 2H_2O$,[5] are lamellar compounds which undergo intercalation reactions with species as diverse as alcohols, pyridine, amides, metal ions, quaternary ammonium salts, and ferrocene.[6] The related layered solid pyrophosphate $[(VO)_2P_2O_7]$ is effective in the catalytic

* To whom correspondence should be addressed.
[†] Syracuse University.
[‡] NEC Research Institute.
[§] University of New Orleans.
[⊗] Abstract published in *Advance ACS Abstracts,* April 15, 1995.

(1) (a) Centi, G.; Trifiro, F.; Ebner, J. R.; Franchett, V. M. *Chem. Rev.* **1988**, *88*, 55. (b) Hodnett, B. L. *Catal. Rev.—Sci. Eng.* **1985**, *27*, 373. (c) Bordes, E.; Courtine, P. *J. Catal.* **1979**, *57*, 236.
(2) Alberti, G. *Acc. Chem. Res.* **1978**, *11*, 163. Clearfield, A. *Chem. Rev.* **1988**, *88*, 125.
(3) Beltran, D.; Beltran, A.; Amoros, P.; Ibañez, R.; Martinez, E.; LeBail, A.; Ferey, G.; Villeneune, G. *Eur. J. Solid State Inorg. Chem.* **1991**, *28*, 131.
(4) Tietze, H. R. *Aust. J. Chem.* **1981**, *34*, 2035.
(5) Johnson, J. W.; Jacobson, A. J.; Brody, J. F.; Lewandowski, J. T. *Inorg. Chem.* **1984**, *23*, 3842. Johnson, J. W.; Jacobson, A. J.; Rich, S. M.; Brody, J. F. *J. Am. Chem. Soc.* **1981**, *103*, 5246. Clearfield, A.; Stynes, J. A. *J. Inorg. Nucl. Chem.* **1964**, *26*, 117. Cao, G.; Hong, H.-G.; Mallouk, T. M. *Acc. Chem. Res.* **1992**, *25*, 420. Dines, M. B.; Griffith, P. C. *Inorg. Chem.* **1983**, *22*, 567. Dines, M. B.; Cooksey, R. E.; Griffith, P. C.; Lane, R. H. *Inorg. Chem.* **1983**, *22*, 1003.

0020-1669/95/1334-3509$09.00/0

air oxidation of butane to maleic anhydride.[2] The interlayer spaces of some of these lamellar solids display characteristics of molecular recognition, in the sense of providing a reaction vessel of molecular dimensions in which the organic substrate is held in the proper orientation for a specific chemical reaction.[7,8] The introduction of other metal cations to produce ternary compositions of the $M^{+n}-V^{+m}-P-O$ system allows a dramatic expansion of the structural chemistry of these phases, giving a variety of lamellar and channel structures with the cations located in the interlamellar regions or occupying the hydrophilic channels.[9-16] The structural types adopted by these phases reflect not only the identity of the cation M^{+n} but the vanadium oxidation state, the pH of the solution, and consequently the degree of protonation of the phosphate residues $(H_nPO_4)^{(3-n)-}$ ($n = 0-2$), and the presence of aquo coligands.

We recently demonstrated that the structural versatility of the oxovanadium phosphate system may be further expanded by the introduction of organoammonium cations to give both three-dimensional frameworks represented by $[(CH_3)_2NH_2]K_4[V_{10}O_{10}(H_2O)_2(OH)_4(PO_4)_7]\cdot 4H_2O$,[17] $(H_3NCH_2CH_2NH_3)_{2.5}[V(H_2O)_2(VO)_8(OH)_4(HPO_4)_4(PO_4)_4(H_2O)_2]\cdot 2H_2O$,[18] $[H_3N(CH_2)_3NH_3]K[(VO)(PO_4)]_3$,[19] $[H_3N(CH_2)_3NH_3][(VO)_3(PO_4)_2(OH)_2(H_2O)_2]$,[20] the newly discovered supercage structures based on the $\{V_5O_9(PO_4)_4\}^{n-}$ cluster core,[21] and two-dimensional phases of the type $(H_2NC_4H_8NH_2)[(VO)_2(PO_4)_2]$ and $(H_2NC_4H_8NH_2)_2[(VO)_3(HPO_4)_2(PO_4)_2]\cdot H_2O$.[22] Since the topology of the inorganic layers of oxovanadium phosphate lamellar materials is strongly influenced by the templating effects of other metal cations or of organoammonium cations which potentially enhance or inhibit interlayer hydrogen-bonding interactions,[23] we sought to investigate the influence of a variety of organoammonium templates on the structures of the V/P/O layers of lamellar phases of the $(R_nN_{4-n})-V-P-O$ family of materials.

While the previously reported examples of this class of materials, $(H_2NC_4H_8NH_2)[(VO)_2(PO_4)_2]$ and $(H_2NC_4H_8NH_2)_2[(VO)_3(HPO_4)_2(PO_4)_2]\cdot H_2O$,[22] exhibited V/P/O layers based on distorted and defect $MOPO_4$ structure types, the compounds of this study $[H_2N(C_4H_8)NH_2][(VO)_4(OH)_4(PO_4)_2]$ (**1**), $[(H_3NC_3H_6)HN(C_2H_4)_2NH(C_3H_6NH_3)][(VO)_5(OH)_2(PO_4)_4]\cdot 2H_2O$ (**2**), $[HN(C_2H_4)_3NH]_2[(VO)_8(OH)_2(HPO_4)_3(PO_4)_4]\cdot 2H_2O$ (**3**), and $[HN(C_2H_4)_3NH][(VO)_3(OH)_2(PO_4)_2]$ (**4**) possess unique connectivities of vanadium polyhedra and phosphate tetrahedra, resulting in structural motifs based on binuclear, trinuclear and tetranuclear oxovanadium clusters, and infinite $\{V-O\cdots V-O\cdots\}$ chains. This paper discusses the syntheses of these four compounds and describes their structural features.

Experimental Section

The hydrothermal reactions were carried out in Parr acid digestion bombs with 23 mL poly(tetrafluoroethylene) liners or in borosilicate tubes with 15 mm outer diameter, 11 mm inner diameter, and length of 254 mm. Phosphoric acid (85 wt % solution), $(CH_3)PO_3H_2$, piperazine, 1,4-bis(aminopropyl)piperazine hydrochloride, 1,4-diazabicyclo[2.2.2]octane (DABCO), tetrabutylammonium hydroxide (40 wt % solution), and VCl_4 were obtained from Aldrich. The VCl_4 was carefully hydrolyzed to generate a turquoise-colored solution of "VO^{2+}" that was used as the vanadium(IV) source. The molarity of these solutions ranged from 0.800 to 2.500 M, depending on reaction requirements. Infrared spectra were obtained on a Perkin-Elmer 1600 Series FTIR spectrometer. For compounds **3** and **4**, the magnetic susceptibility data were recorded using a Quantum Design MPMS-5S SQUID susceptometer.

Synthesis of Compounds. (a) $(H_2N(C_4H_8)NH_2)[(VO)_4(OH)_4(PO_4)_2]$ (1). A mixture of VCl_4, H_3PO_4, piperazine, tetrabutylammonium hydroxide, and H_2O (10 mL, 44% fill volume) in the mole ratio 1:2.2:1.7:1.2:2830 was placed in an acid digestion bomb and heated at 200 °C for 48 h. The pH of the solution at completion was *ca.* 3. Blue plates of **1** were isolated in 65% yield based on vanadium. Similar results were obtained when the reaction was carried out at 150 °C for 110 h. IR (KBr pellet, cm^{-1}): 3480 (m), 2999 (m), 2809 (w), 1605 (s), 1096 (s), 1074 (s), 990 (s), 901 (m), 582 (m), 520 (m), 492 (m).

(b) $[(NH_3C_3H_6)HN(C_2H_4)_2NH(C_3H_6NH_3)][(VO)_5(OH)_2(PO_4)_4\cdot 2H_2O$ (2). A mixture of VCl_4, H_3PO_4, 1,4-bis(aminopropyl)piperazine, and water (8 mL, 35% fill volume) in the mole ratio 1:2.4:6.3:1207 was heated in an acid digestion bomb for 114 h at 150 °C. The pH of the solution, after cooling, was found to be *ca.* 5. Blue plates of compound **2** were obtained in 40% yield (based on vanadium) together with a small amount of gray powder which was removed mechanically by washing. IR (KBr pellet, cm^{-1}): 3547 (sh), 3335 (m), 3010 (n), 2764

(6) (a) Benes, L.; Votinsky, J.; Kalousova, J.; Kilkorka, J. *Inorg. Chim. Acta* **1986**, *114*, 47. (b) Martinez-Lara, M.; Moreno-Real, L.; Jimenez-Lopez, A.; Bruque-Gomez, S.; Rodriquez-Gracia, A. *Mater. Res. Bull.* **1986**, *21*, 13. (c) Johnson, J. W.; Jacobson, A. J. *Angew. Chem.* **1983**, *95*, 422. Antonio, M. R.; Barbour, R. L.; Blum, P. R. *Inorg. Chem.* **1987**, *26*, 1235. (d) Martinez-Lara, M.; Jimenez-Lopez, A.; Moreno-Real, L.; Bruque, S.; Casal, B.; Ruiz-Hitzky, E. *Mater. Res. Bull.* **1985**, *20*, 549. (e) Johnson, J. W.; Jacobson, A. J.; Brody, J. F.; Rich, S. M. *Inorg. Chem.* **1982**, *21*, 1333. (f) Matsubazaski, G.-E.; Ohta, S.; Okimo, S. *Inorg. Chim. Acta* **1991**, *184*, 47.

(7) Szostak, R. *Molecular Sieves Principles of Synthesis and Identification*; Van Nostrand Reinhold: New York, 1989. Whittingham, M. S.; Jacobson, A. J. *Intercalation Chemistry*; Academic Press: New York, 1982. Barrer, R. M. *Zeolites and Clay Minerals as Sorbents and Molecular Sieves*; Academic Press: New York, 1978. Thomas, J. M.; Adams, J. M.; Tennakoon, D. T. B. *Adv. Chem. Ser.* **1977**, *163*, 298-315.

(8) Mallouk, T. E.; Lee, H. *J. Chem. Educ.* **1990**, *67*, 829.

(9) $Zn_2VO(PO_4)_2$: Lii, K. H.; Tsai, H. J. *J. Solid State Chem.* **1991**, *90*, 219. $Cs_2V_3P_4O_{17}$: Lii, K. H.; Wang, Y. P.; Wang, S. L. *J. Solid State Chem.* **1989**, *80*, 127. β-$K_2V_3P_4O_{17}$: Lii, K. H.; Tsai, H. J.; Wang, S. L. *J. Solid State Chem.* **1990**, *87*, 396. $A_2VOP_2O_7$ (A = Cs, Rb): Lii, K. H.; Wang, Y. P.; Chen, Y. B.; Wang, S. L. *J. Solid State Chem.* **1989**, *82*, 239. AVP_2O_7 (A = Li-Cs): Lii, K. H.; Wang, Y. P.; Chen, Y. B.; Wang, S. L. *J. Solid State Chem.* **1990**, *86*, 143 and references therein. $NaVOPO_4$: Lii, K. H.; Li, C. H.; Chen, T. M.; Wang, S. L. *Z. Kristallogr.* **1991**, *197*, 67. $RbV_3P_3O_{17+x}$: Lii, K. H.; Lee, C. S. *Inorg. Chem.* **1990**, *29*, 3298.

(10) $A_{0.5}VOPO_4\cdot xH_2O$ (A = Na, $x = 2.0$; A = K, $x = 1.5$): Wang, S. L.; Kang, H. Y.; Cheng, C. Y.; Lii, K. H. *Inorg. Chem.* **1991**, *30*, 3496. $K_2(VO)_2P_3O_9(OH)_3\cdot 1.124H_2O$: Lii, K. H.; Tsai, H. J. *Inorg. Chem.* **1991**, *30*, 446. $K_2(VO)_3(HPO_4)_4$: Lii, K. H.; Tsai, H. J. *J. Solid State Chem.* **1991**, *91*, 331.

(11) $LiVOPO_4$: Lavrov, A. V.; Nikolaev, V. P.; Sadikov, G. G.; Porai-Koshits, M. A. *Sov. Phys.—Dokl. (Engl. Transl.)* **1982**, *27*, 680.

(12) $NH_4(VO)(HPO_4)$: Lii, K. H.; Wu, N. S.; Chen, B. R. *J. Solid State Chem.* **1992**, *97*, 283.

(13) $Ca_2V(PO_4)HPO_4)_2\cdot H_2O$ and $Ca_2V(PO_4)(P_2O_7)$: Lii, K. H.; Wen, N. S.; Su, C. C.; Chen, B. R. *Inorg. Chem.* **1992**, *31*, 439. $Cs_3V_3P_{12}O_{36}$: Lavrov, A. V.; Nikolaev, V. P.; Sadikov, G. G.; Voitenkov, M. Ya. *Sov. Phys.—Dokl. (Engl. Transl.)* **1981**, *26*, 631. $CsV_2P_5O_{16}$: Klinert, B.; Jansen, M. Z. *Anorg. Allg. Chem.* **1988**, *567*, 87. $Na_3V_2P_3O_{12}$: Delmar, C.; Olazcuage, R.; Cherkaoui, F.; Brochu, R.; LeFlen, G. *C. R. Seances Acad. Sci., Sec. C.* **1978**, *287*, 169.

(14) $[Pb_2V_2VO(PO_4)_4]$: Leclaire, A.; Charden, J.; Grandin, A.; Borel, M. M.; Raveau, B. *J. Solid State Chem.* **1994**, *108*, 291 and references therein.

(15) $[K_3(VO)(V_2O_3)(PO_4)_2(HPO_4)]$: Vaughey, J. T.; Harrison, T. A.; Jacobson, A. J. *J. Solid State Chem.* **1994**, *110*, 305 and references therein.

(16) $(NH_4)(VO_2)(HPO_4)$: Amoros, P.; LeBail, A. *J. Solid State Chem.* **1992**, *97*, 283.

(17) Soghomonian, V.; Chen, Q.; Haushalter, R. C.; Zubieta, J.; O'Connor, C. J. *Science* **1993**, *259*, 1596.

(18) Soghomonian, V.; Chen, Q.; Haushalter, R. C.; Zubieta, J. *Angew. Chem., Int. Ed. Engl.* **1993**, *32*, 610.

(19) Soghomonian, V.; Chen, Q.; Haushalter, R. C.; Zubieta, J. *Chem. Mater.* **1993**, *5*, 1690.

(20) Soghomonian, V.; Chen, Q.; Haushalter, R. C.; Zubieta, J. *Chem. Mater.* **1993**, *5*, 1595.

(21) Mayer, L.; Khan, M. I.; Soghomonian, V.; DeBord, J.; Haushalter, R. C.; Zubieta, J. Unpublished results.

(22) Soghomonian, V.; Haushalter, R. C.; Chen, Q.; Zubieta, J. *Inorg. Chem.* **1994**, *33*, 1700.

(23) Nenoff, T. M.; Harrison, W. T. A.; Gier, T. E.; Calabrese, J. C.; Stucky, G. D. *J. Solid State Chem.* **1993**, *107*, 285.

Table 1. Crystallographic Data for the Structure Determinations of $[H_2N(C_4H_8)NH_2][(VO)_4(OH)_4(PO_4)_2]$ (**1**), $[(NH_3C_3H_6)NH(C_2H_4)_2NH(C_3H_6NH_3)][(VO)_5(OH)_2(PO_4)_4]\cdot 2H_2O$ (**2**), $[HN(C_2H_4)_3NH]_2[(VO)_8(HPO_4)_3(PO_4)_4(OH)_2]\cdot 2H_2O$ (**3**), and $[HN(C_2H_4)_3NH]$ $[(VO)_3(OH)_2(PO_4)_2]$ (**4**)

	1	**2**	**3**	**4**
empirical formula	$C_4H_{16}N_2O_{16}P_2V_4$	$C_{10}H_{34}N_4O_{25}P_4V_5$	$C_{12}H_{37}N_2O_{40}P_7V_8$	$C_6H_{16}N_2O_{13}P_2V_3$
a, Å	10.682(2)	9.433(3)	9.559(2)	12.048(2)
b, Å	8.991(2)	17.799(3)	8.840(2)	6.3470(10)
c, Å	8.951(2)	9.356(1)	24.309(5)	20.249(4)
α, deg		103.83(1)		
β, deg	110.41(3)	91.80(2)	100.07(2)	105.30(3)
γ, deg		95.90(2)		
V, Å^3	805.7(4)	1514.7(6)	2022.5(7)	1493.5(8)
Z	2	2	2	4
space group	$P2_1/c$, No. 14	$P\bar{1}$, No. 2	$P2/n$, No. 13	$P2_1/n$, No. 14
D_{calc}, g/cm^{-3}	2.497	2.159	2.466	2.397
μ, cm^{-1}	25.39	24.72	22.75	21.30
λ (Mo Kα), Å	0.710 73	0.710 73	0.710 73	0.710 73
T, K	233	293	213	213
R^a	0.0569	0.0521	0.0561	0.0567
$R_w{}^b$	0.0766	0.0592	0.0650	0.0679

^{a} $R = \sum||F_o| - |F_c|^2/\sum|F_o|$. ^{b} $R_w = \sum w||F_o| - |F_c|^2/\sum w|F_o|$.

(w), 1119 (m), 1063 (s), 1018 (s), 985 (s), 878 (m), 627 (w), 532 (m), 498 (w).

(c) $[HN(C_2H_4)_3NH]_2[(VO)_8(HPO_4)_3(PO_4)_4(OH)_2]\cdot 2H_2O$ (3). Title compounds **3** and **4** were synthesized from the same starting materials. As noted below, it is possible to optimize the synthesis of each, although compound **3** could not be prepared without producing a small amount of **4** as cocrystallite. In the case of **3**, a mixture of VCl_4, H_3PO_4, 1,4-diazabicyclo[2.2.2]octane (DABCO), and H_2O (10 mL, 44% fill volume) in the mole ratio 1:8.0:4.0:1375 was heated at 200 °C for 72 h in a Parr acid digestion vessel. The final solution pH was found to be 3.0. Blue plates of **3** were isolated in 85% yield. IR (KBr pellet, cm^{-1}): 3431 (w), 3148 (w), 3024 (w), 1072 (s), 999 (s), 970 (s), 660 (m), 558 (m), 479 (m).

(d) $[HN(C_2H_4)_3NH][(VO)_3(OH)_2(PO_4)_2]$ (4). A mixture of VCl_4, H_3PO_4, 1,4-diazabicyclo[2.2.2]octane, and H_2O (6 mL, 26% fill volume) in the mole ratio 1:6.0:4.0:2268 was heated in an acid digestion bomb at 200 °C for 48 h. The final pH of the solution was *ca.* 4. After cooling, dark blue plates of **4** were isolated in 75% yield, contaminated with **3** in *ca.* 25% yield. When the same mixture in a sealed borosilicate tube was ramped at the rate of 0.5 °C/min from 25 to 200 °C and then held at that temperature for 36 h, **4** was obtained in 80% yield as a monophasic product based on vanadium. IR (KBr pellet, cm^{-1}): 3528 (w), 3430 (w), 3024 (w), 2794 (w), 2542 (w), 2476 (w), 1147 (m), 1087 (m), 1054 (m), 988 (s), 961 (s), 934 (s), 758 (w), 610 (m), 583 (w), 512 (w).

X-ray Crystallographic Studies. The experimental X-ray data for **1**−**4** are summarized in Table 1, the atomic coordinates are listed in Tables 2−5, and some selected bond lengths and angles are found in Tables 6−9.

The small size and weak diffraction profiles associated with compound **2** required data collection on a high-flux instrument. Consequently, data were collected on the Rigaku AFC7R rotating-anode diffractometer operating at 18 kW. The crystals of compounds **1**, **3**, and **4** proved of sufficient size and quality to collect data on a conventional sealed-tube system, in this case the Rigaku AFC5S diffractometer. In no case was significant crystal decomposition observed during the course of data collection.

For each of the four studies, data were corrected for Lorentz, polarization, and absorption effects in the usual fashion. Structures **1**, **3**, and **4** were solved by Patterson techniques, while **2** was solved by direct methods; all were refined by full-matrix least-squares using SHELXS-86, SHELXTL, or TEXSAN program packages.[24−27] In all cases, refinement proceeded routinely, and no anomalies in temperature factors or excursions of electron density in the final Fourier maps were observed.

In the case of compound **3**, the P(4) site is disordered about the mirror plane and consequently adopts equal populations on either face of the V(3)−V(3a)−V(4)−V(4a) plane. As the refinement proved unexceptional and the anisotropic temperature factors associated with P(4) were reasonable, the disorder model was judged adequate.

Table 2. Atomic Positional Parameters ($\times 10^4$) and Isotropic Temperature Factors (Å^2 $\times$ 10^3) for $[H_2N(C_2H_4)_2NH_2][(VO)_4(OH)_4(PO_4)_2]$ (**1**)

	x	y	z	U(eq)^a
V(1)	2326(1)	5001(1)	1427(1)	8(1)
V(2)	4913(1)	6841(1)	2466(1)	9(1)
P(1)	2878(1)	2523(2)	−862(2)	7(1)
O(1)	1000(4)	5949(5)	1002(5)	14(1)
O(2)	4766(5)	8601(5)	2427(5)	20(2)
O(3)	1956(4)	3426(5)	2770(5)	12(1)
O(4)	1950(4)	3525(5)	−317(5)	11(1)
O(5)	3579(4)	5985(5)	3302(5)	12(1)
O(6)	3520(4)	6073(5)	545(5)	11(1)
O(7)	3692(4)	1473(5)	455(5)	13(1)
O(8)	6221(4)	6469(5)	1426(5)	13(1)
N(1)	10197(5)	4955(6)	6698(6)	15(1)
C(1)	11226(6)	5628(7)	6100(7)	14(1)
C(2)	10565(6)	6231(8)	4439(7)	17(1)

^{a} Equivalent isotropic U defined as one-third of the trace of the orthogonalized U_{ij} tensor.

Results and Discussion

Synthesis and Infrared Spectroscopy. While the metal oxo unit {M=O} is a fundamental constituent both of "simple" soluble clusters[28] and of complex solid materials,[29] synthetic materials containing such functional groups are dominated by molecular examples, rather than solid state phases. This disparity reflects the tendency of synthetic chemists to study soluble molecular materials which can be prepared and crystallized using previously developed, rational synthetic methodolo-

(24) Calabrese, J. C. PHASE—Patterson Heavy Atom Solution Extractor. Ph.D. Thesis; University of Wisconsin—Madison, 1972. Beurskens, P. T. DIRDIF—Direct Methods for Difference Structures and Automatic Procedure for Phase Extraction and Refinement of Difference Structure Factors. Technical Report 1984/1; Crystallographic Laboratory, Toernooiveld, 6525 Ed Nijmegen, The Netherlands, 1984.

(25) Cromer, D. T.; Waber, J. T. *International Tables for X-ray Crystallography*; Kynoch Press: Birmingham, England, 1974; Vol. IV, Table 2.2A.

(26) Ibers, J. A.; Hamilton, W. C. *Acta Crystallogr.* **1964**, *17*, 781.

(27) Cromer, D. T. *International Tables for X-ray Crystallography*; Kynoch Press: Birmingham, England, 1974; Vol. IV, Table 2.3.1.

(28) Zubieta, J. *Mol. Eng.* **1993**, *3*, 93.

(29) Zubieta, J. *Comments Inorg. Chem.* **1994**, *15*, 193.

Table 3. Atomic Positional Parameters ($\times 10^4$) and Isotropic Temperature Factors ($Å^2 \times 10^3$) for $[(H_3NC_3H_6)NH(C_2H_4)_2NH(C_3H_6NH_3)][(VO)_5(OH)_2(PO_4)_4]\cdot 2H_2O$ (**2**)

atom	*x*	*y*	*z*	B_{eq}[a]
V(1)	0.1135(1)	0.33747(8)	0.3719(1)	1.20(3)
V(2)	0.0822(1)	0.14593(8)	0.2718(1)	1.22(2)
V(3)	0.4583(1)	0.30914(9)	0.8545(1)	1.55(3)
V(4)	−0.2193(2)	0.28628(10)	−0.1451(1)	1.94(3)
V(5)	−0.4177(1)	0.21026(8)	0.3203(1)	0.98(2)
P(1)	0.3079(2)	0.2482(1)	0.1222(2)	1.29(4)
P(2)	−0.1297(2)	0.2073(1)	0.1197(2)	1.55(4)
P(3)	−0.6757(2)	0.2782(1)	0.5250(2)	0.99(3)
P(4)	−0.1136(2)	0.2394(1)	0.5203(2)	1.03(4)
O(1)	−0.1296(6)	0.2205(5)	−0.0367(6)	2.8(1)
O(2)	−0.2830(6)	0.2093(4)	0.1671(6)	2.2(1)
O(3)	−0.5259(5)	0.2733(3)	0.4692(5)	1.4(1)
O(4)	−0.6777(6)	0.2630(4)	0.6796(6)	2.0(1)
O(5)	0.0876(6)	0.4261(3)	0.3826(7)	2.4(1)
O(6)	0.1204(6)	0.0611(3)	0.2736(7)	2.4(1)
O(7)	−0.2621(5)	0.2522(3)	0.4661(5)	1.6(1)
O(8)	−0.0615(5)	0.1660(3)	0.4278(6)	1.4(1)
O(9)	−0.0100(6)	0.3129(3)	0.5262(6)	1.6(1)
O(10)	−0.1253(6)	0.2304(4)	0.6804(5)	1.8(1)
O(11)	−0.3789(6)	0.2983(4)	−0.2690(6)	2.6(1)
O(12)	−0.3843(5)	0.2890(4)	−0.0242(6)	1.7(1)
O(13)	−0.1283(9)	0.3695(5)	−0.0949(9)	5.0(2)
O(14)	0.2782(5)	0.3598(3)	0.5296(5)	1.4(1)
O(15)	−0.0257(6)	0.2683(3)	0.2275(6)	1.7(1)
O(16)	0.2589(6)	0.3213(3)	0.2202(6)	1.6(1)
O(17)	−0.5422(6)	0.2359(4)	0.1738(5)	1.8(1)
O(18)	−0.4610(7)	0.1211(3)	0.3214(6)	2.2(1)
O(19)	0.2033(6)	0.1762(3)	0.1176(6)	1.8(1)
O(20)	0.3178(6)	0.2569(4)	−0.0374(5)	2.2(1)
O(21)	−0.7881(5)	0.2232(3)	0.4194(5)	1.5(1)
O(22)	−0.0776(6)	0.1286(4)	0.1182(6)	2.0(1)
O(23)	0.4419(8)	0.3999(4)	0.8997(8)	3.5(2)
O(24)	0.242(2)	0.4593(8)	0.111(1)	3.6(4)
O(25)	0.644(4)	0.076(2)	0.596(4)	3.6(7)
N(1)	0.0903(8)	0.1571(5)	0.7807(8)	2.5(1)
N(2)	0.4081(10)	0.0109(5)	0.882(1)	3.7(2)
N(3a)	0.132(2)	0.4028(9)	0.803(2)	2.1(2)
N(4a)	0.348(2)	0.5209(8)	0.555(2)	1.9(2)
C(1)	0.114(1)	0.0841(6)	0.672(1)	2.8(2)
C(2)	0.199(2)	0.0328(9)	0.744(2)	5.4(3)
C(3)	0.342(2)	0.0672(9)	0.798(2)	5.7(3)
C(4)	0.350(1)	−0.0012(7)	1.023(1)	4.4(2)
C(5)	0.560(1)	0.0490(8)	0.909(1)	4.6(3)
C(6)	0.119(1)	0.4747(7)	0.788(1)	4.3(2)
C(7a)	0.238(2)	0.535(1)	0.802(2)	3.0(4)
C(8a)	0.269(2)	0.573(1)	0.674(2)	2.5(3)
C(9a)	0.341(2)	0.551(1)	0.419(2)	2.5(3)
C(10a)	0.499(2)	0.520(1)	0.608(2)	2.7(3)
N(3b)	−0.012(2)	0.455(1)	0.742(2)	3.2(3)
N(4b)	0.436(2)	0.5002(9)	0.658(2)	2.7(3)
C(7b)	0.205(2)	0.547(1)	0.758(2)	2.4(3)
C(8b)	0.364(2)	0.553(1)	0.781(2)	3.2(4)
C(9b)	0.429(3)	0.531(1)	0.519(2)	3.6(4)
C(10b)	0.587(2)	0.499(1)	0.705(2)	3.6(4)

[a] $B_{eq} = (8/3)\pi^2(U_{11}(aa^*) + U_{22}(bb^*)^2 + U_{33}(bb^*)^2 + 2U_{12}aa^*bb^* \cos\gamma + 2U_{13}aa^*cc^* \cos\beta + 2U_{23}bb^*cc^* \cos\alpha)$.

Table 4. Atomic Positional Parameters ($\times 10^4$) and Isotropic Temperature Factors ($Å^2 \times 10^3$) for $[HN(C_2H_4)_3NH]_2[(VO)_8(HPO_4)_3(PO_4)_4(OH)_2]\cdot 2H_2O$ (**3**)

	x	*y*	*z*	*U*(eq)[a]
V(1)	7297(1)	3661(1)	5468(1)	13(1)
V(2)	6361(1)	7572(1)	4959(1)	14(1)
V(3)	6005(2)	1257(2)	7129(1)	37(1)
V(4)	9765(2)	5403(2)	7918(1)	30(1)
P(1)	6046(3)	428(2)	5758(1)	22(1)
P(2)	4968(2)	5531(2)	5699(1)	9(1)
P(3)	8710(2)	3481(3)	6807(1)	19(1)
P(4)	7761(4)	−1970(4)	7624(1)	11(1)
O(1)	8799(6)	3933(7)	5302(2)	27(2)
O(2)	7935(6)	7566(7)	4837(2)	28(2)
O(3)	4595(10)	457(9)	7240(3)	48(4)
O(4)	3957(13)	−3877(13)	7263(4)	19(3)
O(5)	5241(6)	3278(6)	6845(2)	22(2)
O(6)	7060(6)	1492(6)	5526(2)	22(2)
O(7)	4507(6)	756(6)	5481(2)	24(2)
O(8)	6467(8)	−1213(6)	5637(2)	37(2)
O(9)	6193(7)	573(6)	6398(2)	32(2)
O(10)	6429(5)	5782(5)	5499(2)	11(1)
O(11)	6098(5)	3490(6)	4691(2)	18(2)
O(12)	9979(5)	6024(6)	8705(2)	15(1)
O(13)	4722(5)	3814(5)	5634(2)	11(1)
O(14)	7693(5)	3805(6)	6279(2)	16(1)
O(15)	8811(12)	4787(8)	7178(3)	70(4)
O(16)	8292(9)	2131(6)	7112(3)	54(3)
O(17)	9995(12)	2550(14)	6605(4)	26(4)
O(18)	7929(11)	9695(10)	7452(5)	44(4)
O(19)	9238(12)	7284(12)	7708(4)	41(4)
O(20)	7199(10)	8011(11)	8208(4)	41(3)
O(21)	6678(12)	7334(13)	7186(4)	44(4)
O(22)	2347(24)	2970(23)	7330(10)	93(12)
O(23)	2138(20)	2449(30)	6339(9)	111(11)
N(1)	7951(10)	1939(13)	4124(3)	64(4)
N(2)	9890(10)	1080(11)	3562(4)	58(4)
C(1)	8695(14)	3487(12)	3927(5)	59(5)
C(2)	9040(11)	1044(10)	4473(4)	39(3)
C(3)	7270(13)	1147(16)	3631(5)	67(5)
C(4)	10082(17)	2906(16)	3786(7)	101(8)
C(5)	9900(13)	265(15)	4148(5)	63(5)
C(6)	8412(11)	1073(17)	3232(4)	67(5)

[a] Equivalent isotropic *U* defined as one-third of the trace of the orthogonalized $\mathbf{U}_{ij}$ tensor.

gies and which can be characterized using conventional analytical techniques, such as mass spectroscopy and high-resolution NMR in solution. In contrast, for solid state synthesis, kinetic control of the reaction parameters is often lost at the elevated temperatures required to achieve convenient reaction rates for the interdiffusion of solid state starting materials. However, by exploiting the techniques of hydrothermal synthesis, phosphate-based solid state metal oxides may be prepared by self-assembly from structurally simple precursors.

The hydrothermal technique not only provides a low-temperature pathway to metastable structures utilizing inorganic molecular units of a desired geometry or composition but also allows the introduction of a variety of inorganic and/or organic cations to act as templates in directing the organization of the network of oxometal polyhedra and phosphate tetrahedra. Layered compounds with alternating inorganic/organic layers of which **1**−**4** are representative have also been obtained by intercalation of organic species into an inorganic host lattice, for example, amines intercalated into clays,[30] organoammonium cations intercalated into transition metal oxides and dichalcogenides,[31] or redox intercalation into $VOPO_4 \cdot xH_2O$ lattices.[6] Direct incorporation of the organic moiety is represented by the zirconium and vanadium organophosphonates and organophosphates[32,33] and by the hydrothermally prepared oxovana-

(30) Whittingham, M. S.; Jacobson, A. J. *Intercalation Chemistry*; Academic Press: New York, 1982. Dines, M. B.; Marrocco, M. In *Extended Linear Chain Compounds*; Miller, J. S., Ed.; Plenum Press: New York, 1982; Vol. 2, pp 1−57. Barrer, R. M. *Zeolites and Clay Minerals as Sorbents and Molecular Sieves*; Academic Press: New York, 1978. Thomas, J. M.; Adams, J. M.; Tennakoon, D. T. B. *Adv. Chem. Ser.* **1977**, *163*, 298−315.

(31) Schollhorn, R.; Schulte-Nolle, T.; Steinhoff, G. *J. Less-Common Met.* **1980**, *71*, 71. Schöllhorn, R.; Klein Reesink, F.; Reimold, R. *J. Chem. Soc., Chem. Commun.* **1979**, *398*. Subba Rao, G. V.; Shafer, M. W. In *Intercalated Layered Materials*; Levy, F., Ed.; D. Reidel Publishing Co.; Dordrecht, The Netherlands, 1979; pp 990−199. Schöllhorn, R. Solvated Intercalation Compounds of Layered Chalcogenide and Oxide Bronzes. In Intercalation Chemistry; Whittingham, M. S., Jacobson, A. J., Eds.; Academic Press: New York, 1982; pp 315−360.

(32) Bhardwaj, C.; Hu, H.; Clearfield, A. *Inorg. Chem.* **1993**, *32*, 4294 and references therein.

Table 5. Atomic Positional Parameters ($\times 10^4$) and Isotropic Temperature Factors ($Å^2 \times 10^3$) for $[HN(C_2H_4)_3NH][(VO)_3(OH)_2(PO_4)_2]$ (**4**)

	x	*y*	*z*	*U*(eq)[a]
V(1)	1001(1)	1299(2)	1914(1)	7(1)
V(2)	1291(1)	4068(2)	3208(1)	11(1)
V(3)	−1261(1)	6583(2)	3299(1)	8(1)
P(1)	1499(2)	6396(3)	1746(1)	7(1)
P(2)	−1190(2)	1627(3)	2703(1)	7(1)
O(1)	91(5)	1479(10)	1188(3)	12(1)
O(2)	1233(5)	3560(10)	3970(3)	14(1)
o(3)	−931(5)	6651(10)	4115(3)	12(1)
o(4)	2456(5)	807(10)	1648(3)	15(1)
o(5)	138(5)	6343(10)	3004(3)	12(1)
o(6)	1081(5)	6249(10)	980(3)	12(1)
O(7)	1221(5)	4392(10)	2100(3)	8(1)
O(8)	2826(5)	6608(10)	1983(3)	10(1)
O(9)	942(5)	8230(10)	2049(3)	8(1)
O(10)	47(5)	1923(9)	2620(3)	8(1)
O(11)	−2037(5)	1637(10)	1992(3)	10(1)
O(12)	−1275(5)	−411(10)	3070(3)	12(1)
O(13)	−1432(5)	3453(10)	3144(3)	10(1)
N(1)	1978(7)	3895(13)	200(4)	19(2)
N(2)	2700(7)	2630(14)	−786(4)	20(2)
C(1)	3278(8)	3828(16)	406(5)	18(2)
C(2)	3693(9)	3546(17)	−248(5)	22(2)
C(3)	1519(9)	1727(16)	−10(5)	21(2)
C(4)	2191(8)	810(16)	−477(5)	17(2)
C(5)	1572(9)	5355(17)	−401(5)	21(2)
C(6)	1788(9)	4261(17)	−1032(5)	22(2)

[a] Equivalent isotropic *U* defined as one-third of the trace of the orthogonalized $\mathbf{U}_{ij}$ tensor.

Table 6. Selected Bond Lengths (Å) and Angles (deg) for $[H_2N(C_2H_4)_2NH_2][(VO)_4(OH)_4(PO_4)_2]$ (**1**)

V(1)−V(2)	3.075(2)	V(1)−O(1)	1.581(4)
V(1)−O(3)	1.984(5)	V(1)−O(4)	1.980(4)
V(1)−O(5)	1.956(4)	V(1)−O(6)	1.971(5)
V(2)−O(2)	1.589(5)	V(2)−O(5)	1.983(5)
V(2)−O(6)	1.966(4)	V(2)−O(8)	1.958(5)
V(2)−O(7A)	1.964(4)	P(1)−O(4)	1.539(5)
P(1)−O(7)	1.524(4)	P(1)−O(3A)	1.535(4)
P(1)−O(8A)	1.530(5)	O(3)−P(1B)	1.535(4)
O(7)−V(2A)	1.964(4)	O(8)−P(1A)	1.530(5)
N(1)−C(1)	1.506(9)	N(1)−C(2A)	1.503(8)
C(1)−C(2)	1.507(8)	C(2)−N(1A)	1.503(8)
V(2)−V(1)−O(1)	114.7(2)	V(2)−V(1)−O(3)	123.3(1)
O(1)−V(1)−O(3)	100.3(2)	V(2)−V(1)−O(4)	120.8(1)
O(1)−V(1)−O(4)	104.7(2)	O(3)−V(1)−O(4)	88.3(2)
V(2)−V(1)−O(5)	39.0(1)	O(1)−V(1)−O(5)	104.5(2)
O(3)−V(1)−O(5)	91.4(2)	O(4)−V(1)−O(5)	150.4(2)
V(2)−V(1)−O(6)	38.6(1)	O(1)−V(1)−O(6)	106.9(2)
O(3)−V(1)−O(6)	152.3(2)	O(4)−V(1)−O(6)	89.6(2)
O(5)−V(1)−O(6)	77.1(2)	V(1)−V(2)−O(2)	117.2(2)
V(1)−V(2)−O(5)	38.4(1)	O(2)−V(2)−O(5)	108.4(3)
V(1)−V(2)−O(6)	38.7(1)	O(2)−V(2)−O(6)	107.0(2)
O(5)−V(2)−O(6)	76.6(2)	V(1)−V(2)−O(8)	118.6(1)
O(2)−V(2)−O(8)	104.0(3)	O(5)−V(2)−O(8)	147.0(2)
O(6)−V(2)−O(8)	88.4(2)	V(1)−V(2)−O(7A)	120.0(1)
O(2)−V(2)−O(7A)	103.0(2)	O(5)−V(2)−O(7A)	89.1(2)
O(6)−V(2)−O(7A)	149.6(2)	O(8)−V(2)−O(7A)	89.5(2)
O(4)−P(1)−O(7)	112.0(3)	O(4)−P(1)−O(3A)	105.9(2)
O(7)−P(1)−O(3a)	107.9(2)	O(4)−P(1)−O(8A)	107.9(3)
O(7)−P(1)−O(8A)	111.5(2)	O(3A)−P(1)−O(8A)	111.7(3)
V(1)−O(3)−P(1B)	132.2(3)	V(1)−O(4)−P(1)	131.8(2)
V(1)−O(5)−V(2)	102.6(2)	V(1)−O(6)−V(2)	102.7(2)
P(1)−O(7)−V(2A)	131.9(3)	V(2)−O(8)−P(1A)	133.7(3)

dium phosphates $(H_2NC_4H_8NH_2)[(VO)_2(PO_4)_2]$ and $(H_2NC_4H_8NH_2)_2$ $[(VO)_3(HPO_4)(PO_4)_2]\cdot 2H_2O$, previously reported by us.[22]

Table 7. Selected Bond Lengths (Å) and Angles (deg) for $[(H_3NC_3H_6)NH(C_2H_4)_2NH(C_3H_6NH_3)][(VO)_5(OH)_2(PO_4)_4]\cdot 2H_2O$ (**2**)

V(1)−O(5)	1.600(6)	V(1)−O(9)	1.983(5)
V(1)−O(14)	2.048(5)	V(1)−O(15)	1.956(5)
V(1)−O(16)	1.997(5)	V(2)−O(6)	1.592(6)
V(2)−O(8)	2.018(5)	V(2)−O(19)	2.006(6)
V(2)−O(21)	1.983(5)	V(2)−O(22)	1.998(5)
V(3)−O(4)	2.002(6)	V(3)−O(11)	1.948(6)
V(3)−O(12)	1.954(5)	V(3)−O(20)	1.981(6)
V(3)−O(23)	1.594(7)	V(4)−O(1)	1.958(6)
V(4)−O(10)	1.984(5)	V(4)−O(11)	1.931(6)
V(4)−O(12)	1.950(5)	V(4)−O(13)	1.592(7)
V(5)−O(2)	1.943(5)	V(5)−O(3)	1.954(5)
V(5)−O(7)	1.933(5)	V(5)−O(17)	1.942(5)
V(5)−O(18)	1.600(6)	P(1)−O(16)	1.525(6)
P(1)−O(17)	1.534(5)	P(1)−O(19)	1.526(6)
P(1)−O(20)	1.542(5)	P(2)−O(1)	1.536(6)
P(2)−O(2)	1.528(6)	P(2)−O(15)	1.534(6)
P(2)−O(22)	1.528(6)	P(3)−O(3)	1.525(5)
P(3)−O(4)	1.534(5)	P(3)−O(14)	1.550(6)
P(3)−O(21)	1.523(5)	P(4)−O(7)	1.532(5)
P94)−O(8)	1.523(6)	P(4)−O(9)	1.538(6)
P(4)−O(10)	1.550(5)		
O(5)−V(1)−O(9)	100.9(3)	O(5)−V(1)−O(14)	97.1(3)
O(5)−V(1)−O(15)	109.5(3)	O(5)−V(1)−O(16)	101.5(3)
O(9)−V(1)−O(14)	86.3(2)	O(9)−V(1)−O(15)	87.0(2)
O(9)−V(1)−O(16)	157.4(2)	O(14)−V(1)−O(15)	153.4(2)
O(14)−V(1)−O(16)	87.8(2)	O(15)−V(1)−O(16)	88.6(2)
O(6)−V(2)−O(8)	102.9(3)	O(6)−V(2)−O(19)	104.1(3)
O(6)−V(2)−O(21)	108.4(3)	O(6)−V(2)−O(22)	105.0(3)
O(8)−V(2)−O(19)	153.0(2)	O(8)−V(2)−O(21)	84.3(2)
O(8)−V(2)−O(22)	88.8(2)	O(19)−V(2)−O(21)	86.8(2)
O(19)−V(2)−O(22)	84.7(2)	O(21)−V(2)−O(22)	146.5(2)
O(4)−V(3)−O(11)	91.3(2)	O(4)−V(3)−O(12)	144.5(3)
O(4)−V(3)−O(20)	74.5(2)	O(4)−V(3)−O(23)	106.3(3)
O(11)−V(3)−O(12)	73.6(2)	O(11)−V(3)−O(20)	146.3(3)
O(11)−V(3)−O(23)	106.0(4)	O(12)−V(3)−O(20)	90.8(2)
O(12)−V(3)−O(23)	108.7(3)	O(20)−V(3)−O(23)	107.3(3)
O(1)−V(4)−O(10)	86.3(2)	O(1)−V(4)−O(11)	147.7(3)
O(1)−V(4)−O(12)	91.4(2)	O(1)−V(4)−O(13)	105.3(4)
O(10)−V(4)−O(11)	91.0(2)	O(10)−V(4)−O(12)	147.5(3)
O(10)−V(4)−O(13)	104.8(3)	O(11)−V(4)−O(12)	74.0(2)
O(11)−V(4)−O(13)	106.5(4)	O(12)−V(4)−O(13)	107.1(3)
O(2)−V(5)−O(3)	146.7(3)	O(2)−V(5)−O(7)	88.8(2)
O(2)−V(5)−O(17)	81.5(2)	O(2)−V(5)−O(18)	106.1(3)
O(3)−V(5)−O(7)	82.2(2)	O(3)−V(5)−O(17)	86.9(2)
O(3)−V(5)−O(18)	107.2(3)	O(7)−V(5)−O(17)	143.6(3)
O(7)−V(5)−O(18)	108.2(3)	O(17)−V(5)−O(18)	108.2(3)
O(16)−P(1)−O(17)	110.8(3)	O(16)−P(1)−O(19)	111.6(3)
O(16)−P(1)−O(20)	110.2(3)	O(17)−P(1)−O(19)	110.2(3)
O(17)−P(1)−O(20)	106.5(3)	O(19)−P(1)−O(20)	107.3(3)
O(1)−P(2)−O(2)	107.0(3)	O(1)−P(2)−O(15)	111.8(4)
O(1)−P(2)−O(22)	109.6(4)	O(2)−P(2)−O(15)	111.7(3)
O(2)−P(2)−O(22)	110.9(4)	O(15)−P(2)−O(22)	105.8(3)
O(3)−P(3)−O(4)	109.7(3)	O(3)−P(3)−O(14)	110.0(3)
O(3)−P(3)−O(21)	112.2(3)	O(4)−P(3)−O(14)	110.0(3)
O(4)−P(3)−O(21)	111.4(3)	O(14)−P(3)−O(21)	103.4(3)
O(7)−P(4)−O(8)	112.4(3)	O(7)−P(4)−O(9)	108.8(3)
O(7)−P(4)−O(10)	107.1(3)	O(8)−P(4)−O(9)	112.5(3)
O(8)−P(4)−O(10)	108.2(3)	O(9)−P(4)−O(10)	107.5(3)
V(4)−O(1)−P(2)	137.2(4)	V(5)−O(2)−P(2)	149.3(3)
V(5)−O(3)−P(3)	142.0(3)	V(3)−O(4)−P(3)	128.7(4)
V(5)−O(7)−P(4)	144.3(4)	V(2)−O(8)−P(4)	133.8(3)
V(1)−O(9)−P(4)	129.0(3)	V(4)−O(10)−P(4)	133.9(3)
V(3)−O(11)−V(4)	106.5(3)	V(3)−O(12)−V(4)	105.6(2)
V(1)−O(14)−P(3)	103.6(3)	V(1)−O(15)−P(2)	174.3(4)
V(1)−O(16)−P(1)	132.7(3)	V(5)−O(17)−P(1)	149.2(3)
V(2)−O(19)−P(1)	131.5(3)	V(3)−O(20)−P(1)	135.6(4)
V(2)−O(21)−P(3)	174.0(4)	V(2)−O(22)−P(2)	108.2(3)

The syntheses of **1**−**4** used a hydrolyzed solution of VCl_4 as the vanadium source. The vanadium is present as V(IV), as deduced by redox titration,[34] and presumably exists as hydrated

(33) Khan, M. I.; Lee, Y. J.; O'Connor, C. J.; Haushalter, R. C.; Zubieta, J. *J. Am. Chem. Soc.* **1994**, *116*, 4525.

(34) Hentz, F. C., Jr.; Long, G. G. *J. Chem. Educ.* **1978**, *55*, 55. Long, G. G.; Stanfield, R. L.; Hentz, F. C., Jr. *J. Chem. Educ.* **1979**, *56*, 195.

Table 8. Selected Bond Lenghts (Å) and Angles (deg) for $[HN(C_2H_4)_3NH]_2[(VO)_8(HPO_4)_3(PO_4)_4(OH)_2]\cdot 2H_2O$ (**3**)

V(1)−P(2)	2.906(2)	V(1)−O(1)	1.576(6)
V(1)−O(6)	1.939(5)	V(1)−O(10)	2.057(5)
V(1)−O(11)	2.036(5)	V(1)−O(14)	1.946(5)
V(2)−O(2)	1.583(6)	V(2)−O(10)	2.049(5)
V(2)−O(7a)	1.925(5)	V(2)−O(8a)	1.956(6)
V(2)−O(13a)	2.032(4)	V(3)−O(3)	1.587(10)
V(3)−O(5)	2.006(6)	V(3)−O(9)	1.941(6)
V(3)−O(16)	2.326(8)	V(3)−V(3b)	3.101(3)
V(3)−O(18a)	2.324(10)	V(4)−O(12)	1.966(5)
V(4)−O(15)	1.945(7)	V(4)−O(19)	1.787(10)
V(4)−O(4a)	1.510(12)	V(4)−O(5a)	1.965(6)
P(1)−O(6)	1.528(6)	P(1)−O(7)	1.534(6)
P(1)−O(8)	1.546(6)	P(1)−O(9)	1.517(5)
P(2)−O(10)	1.573(5)	P(2)−O(13)	1.540(5)
P(2)−O(11a)	1.532(5)	P92)−O(12a)	1.506(5)
P(3)−O(14)	1.497(5)	P(3)−O(15)	1.458(7)
P(3)−O(16)	1.495(7)	P(3)−O(17)	1.624(12)
P(4)−O(18a)	1.546(10)	P(4)−O(19a)	1.539(12)
P(4)−O(20a)	1.602(11)	P(4)−O(21a)	1.482(11)
O(4)−V(4a)	1.510(12)	O(5)−V(4b)	1.965(6)
O(7)−V(2b)	1.925(5)	O(8)−V(2a)	1.956(6)
O(1)−V(1)−O(6)	107.0(3)	O(1)−V(1)−O(10)	105.2(3)
O(6)−V(1)−O(10)	147.8(2)	O(1)−V(1)−O(11)	99.5(2)
O96)−V(1)−O(11)	86.6(2)	O(10)−V(1)−O(11)	86.4(2)
O(1)−V(1)−O(14)	103.0(2)	O(6)−V(1)−O(14)	89.7(2)
O(10)−V(1)−O(14)	84.9(2)	O(11)−V(1)−O(14)	157.4(2)
O(2)−V(2)−O(10)	101.1(3)	O(2)−V(2)−O(7a)	103.3(3)
O(10)−V(2)−O(7a)	155.6(2)	O(2)−V(2)−O(8a)	104.4(3)
O(10)−V(2)−O(8a)	83.9(2)	O(7A)−V(2)−O(8a)	90.0(2)
O(2)−V(2)−O(13a)	104.4(3)	O(10)−V(2)−O(13a)	86.8(2)
O(7a)−V(2)−O(13a)	87.3(2)	O(8a)−V(2)−O(13a)	150.9(3)
O(3)−V(3)−O(5)	100.7(4)	O(3)−V(3)−O(9)	103.8(3)
O(5)−V(3)−O(9)	92.6(2)	O(3)−V(3)−O(16)	168.6(3)
O(5)−V(3)−O(16)	89.1(2)	O(9)−V(3)−O(16)	81.2(3)
O(12)−V(4)−O(15)	158.3(4)	O(12)−V(4)−O(19)	89.7(4)
O(15)−V(4)−O(19)	86.2(4)	O(12)−V(4)−O(4a)	102.3(4)
O(15)−V(4)−O(4a)	96.9(5)	O(19)−V(4)−O(4a)	74.1(6)
O(12)−V(4)−O(5a)	89.2(2)	O(15)−V(4)−O(5a)	88.8(2)
O(19)−V(4)−O(5a)	163.5(4)	O(4a)−V(4)−O(5a)	122.2(5)
O(6)−P(1)−O(7)	110.1(3)	O(6)−P(1)−O(8)	107.7(4)
O(7)−P(1)−O(8)	110.8(3)	O(6)−P(1)−O(9)	111.5(3)
O(7)−P(1)−O(9)	109.9(4)	O(8)−P(1)−O(9)	106.8(3)
O(10)−P(2)−O(13)	103.6(3)	V(1)−P(2)−O(11a)	130.6(2)
O(10)−P(2)−O(11a)	105.0(3)	O(13)−P(2)−O(11a)	114.8(3)
O(10)−P(2)−O(12a)	112.0(3)	O(13)−P(2)−O(12a)	111.3(3)
O(11a)−P(2)−O(12a)	109.9(3)	O(14)−P(3)−O(15)	110.0(4)
O(14)−P(3)−O(16)	112.8(4)	O(15)−P(3)−O(16)	108.6(4)
O(14)−P(3)−O(17)	104.4(4)	O(15)−P(3)−O(17)	128.1(6)
O(16)−P(3)−O(17)	101.5(5)	O(18a)−P(4)−O(19a)	107.9(6)
O(18)−P(4)−O(20a)	108.4(6)	O(19a)−P(4)−O(20a)	108.7(6)
O(18a)−P(4)−O(21a)	107.1(6)	O(19a)−P(4)−O(21a)	115.2(6)
O(20a)−P(4)−O(21a)	109.3(6)	V(3)−O(5)−V(4b)	140.3(2)
V(1)−O(6)−P(1)	136.5(4)	P(1)−O(7)−V(2b)	132.5(3)
P(1)−O(8)−V(2a)	134.3(3)	V(3)−O(9)−P(1)	163.0(4)
V(1)−O(10)−V(2)	130.4(3)	V(1)−O(10)−P(2)	105.6(3)
V(2)−O(10)−P(2)	112.1(3)	V(1)−O(11)−P(2a)	137.6(3)
V(4)−O(12)−P(2b)	146.7(3)	P(2)−O(13)−V(2b)	135.8(3)
V(1)−O(14)−P(3)	147.1(3)	V(4)−O(15)−P(3)	139.7(5)
V(3)−O(16)−P(3)	127.4(4)	V(3)−O(16)−V(3b)	91.1(3)
P(3)−O(16)−V(3b)	133.5(4)	V(3a)−O(18)−P(4a)	122.9(6)
V(3C)−O(18)−P(4a)	128.1(7)	V(4)−O(19)−P(4a)	130.0(7)
V(4b)−O(21)−P(4a)	139.1(7)		

Table 9. Selected Bond Lengths (Å) and Angles (deg) for $[HN(C_2H_4)_3NH][(VO)_3(OH)_2(PO_4)_2]$ (**4**)

V(1)−O(1)	1.589(5)	V(1)−O(4)	1.980(7)
V(1)−O(7)	2.003(6)	V(1)−O(10)	2.095(7)
V(1)−O(8a)	2.315(6)	V(1)−O(9a)	1.971(6)
V(2)−O(2)	1.596(7)	V(2)−O(5)	1.971(6)
V(2)−O(7)	2.233(6)	V(2)−O(10)	2.140(6)
V(2)−O(4a)	1.869(7)	V(2)−O(8a)	1.984(7)
V(3)−O(3)	1.595(6)	V(3)−O(5)	1.936(7)
V(3)−O(13)	2.013(6)	V(3)−O(11a)	1.979(6)
V(3)−O(12a)	1.962(6)	P(1)−O(6)	1.501(6)
P(1)−O(7)	1.539(7)	P(1)−O(8)	1.549(6)
P(1)−O(9)	1.548(7)	P(2)−O(10)	1.554(7)
P(2)−O(11)	1.529(6)	P(2)−O(12)	1.509(7)
P(2)−O(13)	1.538(7)	O(4)−V(2a)	1.869(7)
O(8)−V(1b)	2.315(6)	O(8)−V(2b)	1.984(7)
O(9)−V(1a)	1.971(6)	O(11)−V(3b)	1.979(6)
O(16)−V(3a)	1.962(6)	N(1)−C(1)	1.511(12)
N(1)−C(3)	1.502(13)	N(1)−C(5)	1.505(13)
N(2)−C(2)	1.506(12)	N(2)−C(4)	1.518(14)
N(2)−C(6)	1.496(13)	C(1)−C(2)	1.545(16)
C(3)−C(4)	1.515(16)	C(5)−C(6)	1.535(16)
O(1)−V(1)−O(4)	101.7(3)	O(1)−V(1)−O(7)	97.4(3)
O(4)−V(1)−O(7)	95.3(3)	O(1)−V(1)−O(10)	104.4(3)
O(4)−V(1)−O(10)	153.3(2)	O(7)−V(1)−O(10)	75.8(3)
O(1)−V(1)−O(8a)	169.4(3)	O(4)−V(1)−O(8a)	85.1(2)
O(7)−V(1)−O(8a)	73.6(2)	O(10)−V(1)−O(8a)	68.3(2)
O(1)−V(1)−O(9a)	99.1(3)	O(4)−V(1)−O(9a)	88.9(3)
O(7)−V(1)−O(9a)	161.8(2)	O(10)−V(1)−O(9a)	92.6(3)
O(8a)−V(1)−O(9a)	89.1(2)	O(2)−V(2)−O(5)	98.2(3)
O(2)−V(2)−O(7)	172.2(3)	O(5)−V(2)−O(7)	83.4(2)
O(2)−V(2)−O(10)	102.0(3)	O(5)−V(2)−O(10)	89.9(2)
O(7)−V(2)−O(10)	70.3(2)	O(2)−V(2)−O(4a)	102.5(3)
O(5)−V(2)−O(4a)	94.1(3)	O(7)−V(2)−O(4a)	85.0(3)
O(10)−V(2)−O(4a)	154.4(3)	O(2)−V(2)−O(8a)	101.1(3)
O(5)−V(2)−O(8a)	157.0(2)	O(7)−V(2)−O(8a)	75.9(2)
O(10)−V(2)−O(8a)	73.9(2)	O(4a)−V(2)−O(8a)	94.0(3)
O(3)−V(3)−O(5)	108.8(3)	O(3)−V(3)−O(13)	100.1(3)
O(5)−V(3)−O(13)	86.3(3)	O(3)−V(3)−O(11a)	105.3(3)
O(5)−V(3)−O(11a)	145.8(3)	O(13)−V(3)−O(11a)	85.1(2)
O(3)−V(3)−O(12a)	101.7(3)	O(5)−V(3)−O(12a)	87.6(3)
O(13)−V(3)−O(12a)	158.1(3)	O(11a)−V(3)−O(12a)	88.2(3)
O(6)−P(1)−O(7)	112.0(3)	O(6)−P(1)−O(8)	111.2(4)
O(7)−P(1)−O(8)	105.1(3)	O(6)−P(1)−O(9)	113.2(3)
O(7)−P(1)−O(9)	105.5(4)	O(8)−P(1)−O(9)	109.4(3)
O(10)−P(2)−O(11)	108.6(4)	O(10)−P(2)−O(12)	110.4(4)
O(11)−P(2)−O(12)	110.6(3)	O(10)−P(2)−O(13)	107.8(3)
O(11)−P(2)−O(13)	111.2(3)	O(12)−P(2)−O(13)	108.2(4)
V(1)−O(4)−V(2a)	140.6(4)	V(2)−O(5)−V(3)	128.0(3)
V(1)−O(7)−V(2)	93.9(3)	V(1)−O(7)−P(1)	139.1(4)
V(2)−O(7)−P(1)	126.1(3)	P(1)−O(8)−V(1b)	127.5(4)
P(1)−O(8)−V(2b)	124.8(4)	V(1b)−O(8)−V(2b)	91.9(2)
P(1)−O(9)−V(1a)	130.7(4)	V(1)−O(10)−V(2)	94.0(2)
V(1)−O(10)−P(2)	139.9(3)	V(2)−O(10)−P(2)	124.6(4)
P(2)−O(11)−V(3b)	131.5(4)	P(2)−O(12)−V(3a)	162.3(5)
V(3)−O(13)−P(2)	143.8(4)		

VO^{2+} groups. The use of a reduced vanadium precursor is essential in order to avoid the formation of mixed-valence clusters of the $[V_{15}O_{36}X]^{6-}$ class.[35]

The reaction of VCl_4, H_3PO_4, tetrabutylammonium hydroxide, piperazine, and H_2O in the mole ratio 1:2.2:1.7:1.2:2830 heated at 200 °C for 48 h yields $(H_2NC_4H_8NH_2)][(VO)_4(OH)_4(PO_4)_2]$ (**1**) as blue plates in 65% yield. Optimization of reaction conditions revealed that $(n\text{-}C_4H_9)_4NOH$ was the most effective reagent in adjusting the solution pH to the 3−6 range, a requirement for the isolation of **1**. When 1,4-diaminopiperazine hydrochloride is used as the templating reagent and the reaction is carried out in Parr bombs, compound **1** is also obtained as a monophasic material in high yield. This observation is consistent with the degradation of the 1,4-diaminopiperazine to piperazine and ammonia by protonation and N−N bond cleavage. Similar amine cleavage reactions have been observed in the preparations of other oxovanadium phosphate and organophosphonate phases.[36] Curiously, when 1,4-diaminopiperazine is used in the same reaction in borosilicate tubes, a novel three-dimensional framework material $(H_2N(C_4H_8)NH_2)[(VO)_4$-

(35) Müller, A.; Penk, M.; Rohlfing, R.; Krickemeyer, E.; Döring, J. *Angew. Chem., Int. Ed. Engl.* **1990**, *29*, 926.

(36) Soghomonian, V.; Chen, Q.; Haushalter, R. C.; Zubieta, J. *Angew. Chem., Int. Ed. Engl.*, in press.

$(HPO_4)_2(PO_4)_2(H_2O)_4$] is obtained,[37] again via degradation of the precursor amine to the piperazinium cation.

When the piperazine derivative 1,4-bis(3-aminopropyl)-piperazine is employed in the reaction with VCl_4, H_3PO_4, and water at 150 °C for 114 h, the compound $[(H_3NC_3H_6)NH(C_2H_4)_2$-$NH(C_3H_6NH_3)][(VO)_5(OH)_2(PO_4)_4]\cdot 2H_2O$ (**2**) is obtained as blue plates in 40% yield. Under the acidic reaction conditions, the template is fully protonated and appears as the +4 cation in the product.

While the syntheses of **3** and **4** employ the same template, 1,4-diazabicyclo[2.2.2]octane (DABCO), and the same vanadium and acid reagents, variations in stoichiometries of these precursors result in the two unique structural types. It is a curious feature of the templating mechanism, which remains somewhat enigmatic, that the same template can give rise to dramatically different structures. While charge-compensating and space-filling effects contribute to the process, other factors, such as pH, temperature, and stoichiometry are clearly important.

The infrared spectroscopy of **1**−**4** exhibits characteristic primary and secondary ν(N−H) stretching modes in the 3500−3000 cm^{-1} region. A series of three bands of medium to strong intensity in the 1200−1000 cm^{-1} range appears in all cases and is attributed to ν(P−O). Strong bands in the 960−990 cm^{-1} region are assigned to ν(V=O) for vanadium in the +4 oxidation state.

X-Ray Structural Studies. While compounds **1**−**4** are members of class of layered compounds characterized by alternating inorganic/organic layers, the details of the polyhedral connectivities defining the V/P/O networks of the inorganic layers are quite distinctive for each. Furthermore, in contrast to the original examples of 2-D layered oxovanadium/phosphate/organoammonium phases, $(H_2NC_4H_8NH_2)[(VO)_2(PO_4)_2]$ and $(H_2NC_4H_8NH_2)[(VO)_3(HPO_4)_2(PO_4)_2]\cdot 2H_2O$, whose structures may be described as distorted or defected examples of the prototypical $MOPO_4$ layer structure, compounds **1**−**4** exhibit more complex patterns of polyhedral connectivities within the inorganic layers.

As shown in Figure 1a, the fundamental structural motif associated with the V−P−O plane of **1** is the binuclear unit of edge-sharing $\{VO_5\}$ square pyramids. The coordination at each vanadium center is defined by the terminal oxo group, two oxygen donors from each of two μ_3-phosphate groups, and two bridging hydroxy groups. The average V−O(5) and V−O(6) distances of 1.97 Å associated with these latter ligands identifies them as bridging −OH groups, an observation also consistent with the charge requirements of the structure. This binuclear unit is propagated in the layer construction by linkage through the μ_4-PO_4 group, which serves to connect four adjacent $\{V_2O_{10}\}$ moieties. The structure of **1** is reminiscent of the layered $[VOPO_4]$ prototype and may be constructed from that of $VO(PO_4)$ by expansion of the plane through insertion of a $\{VO(OH)_2\}$ unit into a *cis* $\{V(OPO_3)_2\}$ motif at each vanadium site of the layer. In addition to this expansion of the layer motif, **1** contrasts with $[VOPO_4]$ through the introduction of organic cations which occupy the interlamellar regions and exhibit strong hydrogen bonding of the ammonium protons to the vanadyl oxygens of the inorganic layers.

While the previously described layered materials $(H_2NC_4H_8$-$NH_2)[(VO)_2(PO_4)_2]$ and $(H_2NC_4H_8NH_2)[(VO)_3(HPO_4)_2(PO_4)_2]\cdot$ H_2O contain the same piperazinium template as **1**, the V/P/O layer structures are quite distinct. Since $(H_2NC_4H_8NH_2)[(VO)_2$-$(PO_4)_2]$ exhibits isolated $\{VO_5\}$ square pyramids, that is, an absence of V−O−V interactions, and $(H_2NC_4H_8NH_2)[(VO)_3$-$(HPO_4)_2(PO_4)_2]\cdot H_2O$ is characterized by isolated $\{VO_6\}$ octahedra, the presence of corner-sharing V−O(H)−V interactions in **1** results in binuclear cluster sites as the building blocks. The

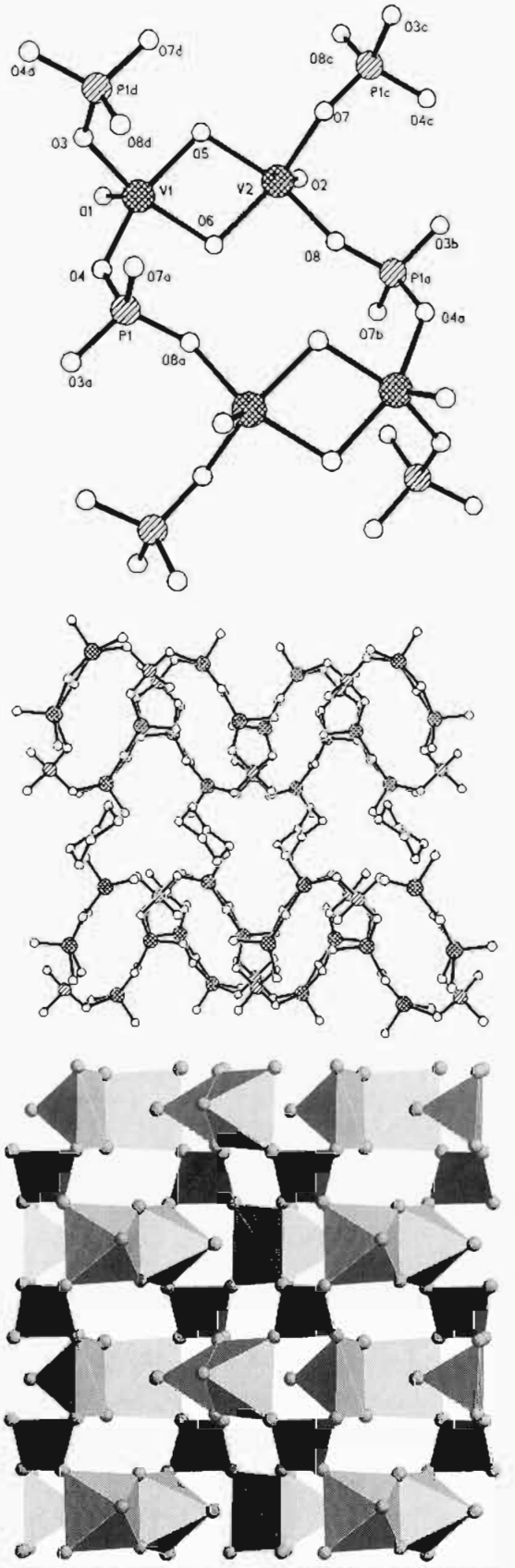

Figure 1. (a) Top: View of the structural building block of **1**, showing the atom-labeling scheme. (b) Middle: View of the positions of the $[H_2N(C_2H_4)_2NH_2]^{2+}$ cations in the interlamellar region. (c) Bottom: Polyhedral representation of the V−P−O layer of **1**.

(37) Soghomonian, V.; Chen, Q.; Haushalter, R. C.; Zubieta, J. Unpublished results.

compositional range of the materials is also noteworthy: V:P ratios of 1:1, 3:4, and 2:1 for $(H_2NC_4H_8NH_2)[(VO)_2(PO_4)_2]$, $(H_2NC_4H_8NH_2)_2[(VO)_3(HPO_4)_2(PO_4)_2]\cdot H_2O$, and **1**, respectively.

The structural motif defining the V/P/O plane of **2** is considerably more complex than that described for **1**. As shown in Figure 2a, **2** possesses two distinct binuclear vanadium sites and a unique mononuclear center which serves as the hinge for the connectivity of polyhedra within the plane. Vanadium centers V(3) and V(4) are present in a binuclear $\{V_2O_{10}\}$ unit of edge-sharing square pyramids reminiscent of the binuclear core of **1**. In a fashion akin to that of **1**, each vanadium is coordinated to a terminal oxo group, two oxygen donors from each of two phosphate groups, and two bridging hydroxy groups. The average V−O(11) and V−O(12) distance of 1.95 Å is similar to that observed for **1** and consistent with protonation of the oxygen sites. The second binuclear site is unprecedented for V/P/O phases and consists of two $\{VO_5\}$ square pyramids symmetrically bridged in the bidentate mode by four PO_4^{3-} groups to produce a copper acetate-type core $\{V_2(\mu_2\text{-}PO_4)_4\}$. This results in a base to base alignment of the vanadium square pyramids associated with V(1) and V(2), with the terminal oxo groups directed along the V···V vector (V(1)···V(2) = 3.075-(1) A). The final vanadium site V(5) consists of an isolated square pyramid, defined by a terminal oxo group and four oxygen donors from each of the four phosphate groups.

The phosphate groups adopt the μ_4-coordination mode, such that each symmetrically bridges a V(1)/V(2) binuclear site and links this site to the V(5) center through one oxygen donor and to the V(3)/V(4) site through the fourth oxygen. The polyhedral view of Figure 2b demonstrates the complexity of the resultant connectivity pattern. The V(5) site is seen to link through the phosphate tetrahedra to two adjacent V(1)/V(2) binuclear sites and to two neighboring V(3)/V(4) binuclear sites. The result is a layer three polyhedra in thickness, as shown in Figure 2c. The organic cations and the water molecules of crystallization occupy the interlamellar regions. Once again, there is significant hydrogen bonding between the ammonium hydrogen atoms and the vanadyl oxygens. Alternate cation layers exhibit terminal $-NH_3^+$ groups directed toward the phosphate oxygens forming the perimeter of the grooves in the V/P/O layer defined by axes of alignment of the V(3)/V(4) binuclear sites. As shown in Figure 2d, the arrangement aligns the $-NH_3^+$ groups with the centers of the 16-membered rings generated by the linkage of pairs of adjacent V(3)/V(4) and V(1)/V(2) binuclear sites.

As shown in Figure 3a,b the structure of the V/P/O layer of **3** exhibits two distinct motifs, best described as dimers of binuclear units. The first unit **3a** consists of two **face-sharing** $\{VO_6\}$ octahedra, each in turn linked via corner-sharing through a bridging −OH group to a square pyramidal $\{VO_5\}$ site. The common face of V(3)/V(3a) octahedra consists of three oxygen donors from each of three phosphate groups. The remaining octahedral coordination sites are defined by a terminal oxo group, the bridging hydroxy group, and the oxygen donor of a fourth phosphate group. The square pyramidal center V(4) enjoys coordination to a terminal oxo group, a bridging hydroxy group, and oxygen donors from each of three phosphate ligands. The O(5) site is again identified as a bridging −OH group by the average V−O distance of 1.98 Å.

The second dimer of dimers motif **3b** may be described as two binuclear units of corner-sharing $\{VO_5\}$ square pyramids linked by two symmetrically bridging phosphate groups. In this way, **3b** consists of a $\{V_4P_2O_6\}$ ring, while **3a** exhibits a $\{V_4PO_5\}$ ring. The vanadium sites associated with unit **3b** exhibit square pyramidal geometry exclusively, with each vanadium bonded to a terminal oxo group, the bridging oxygen donor of the P(2) phosphate group, and three oxygen donors from each of the phosphate groups.

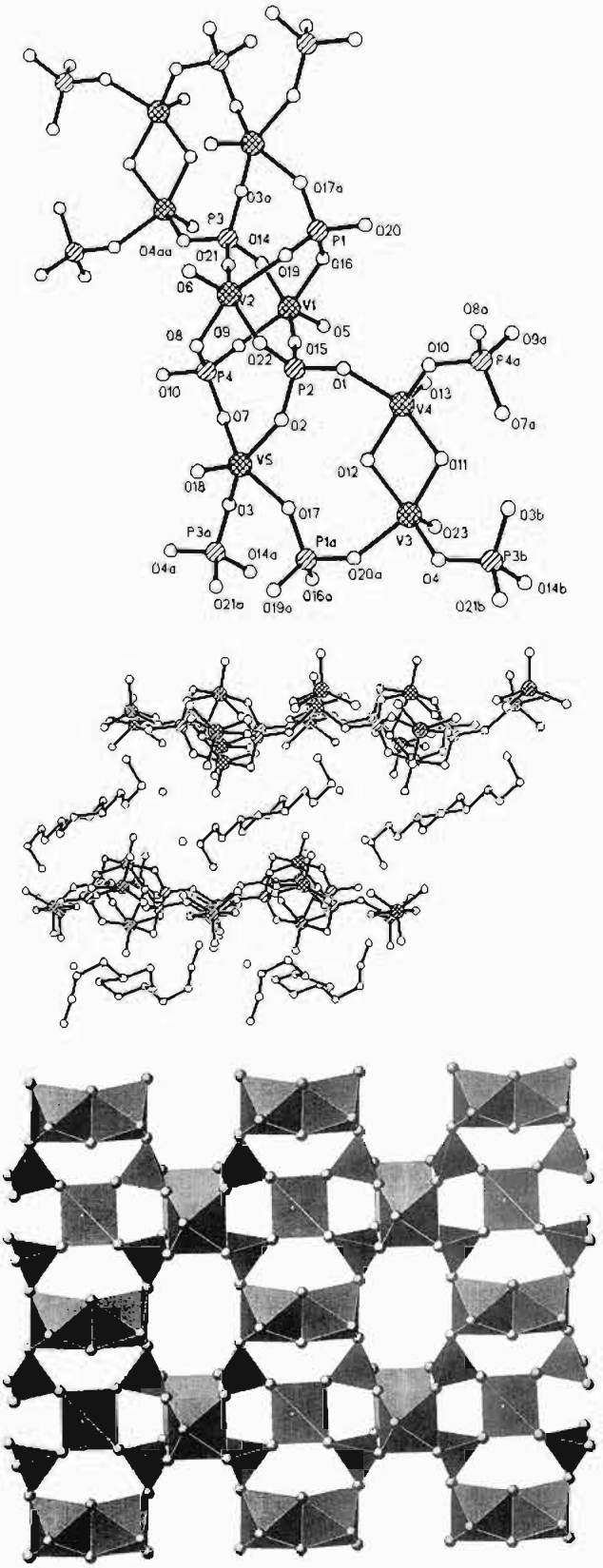

Figure 2. (a) Top: View of the structural building blocks of **2**, showing the atom-labeling scheme. (b) Middle: Representation of the location of the organic cations and water molecules of crystallization in the region between V−P−O layers, giving rise to the characteristic alternation of inorganic and organic layers. (c) Bottom: Polyhedral representation of the V−P−O layer of **2**.

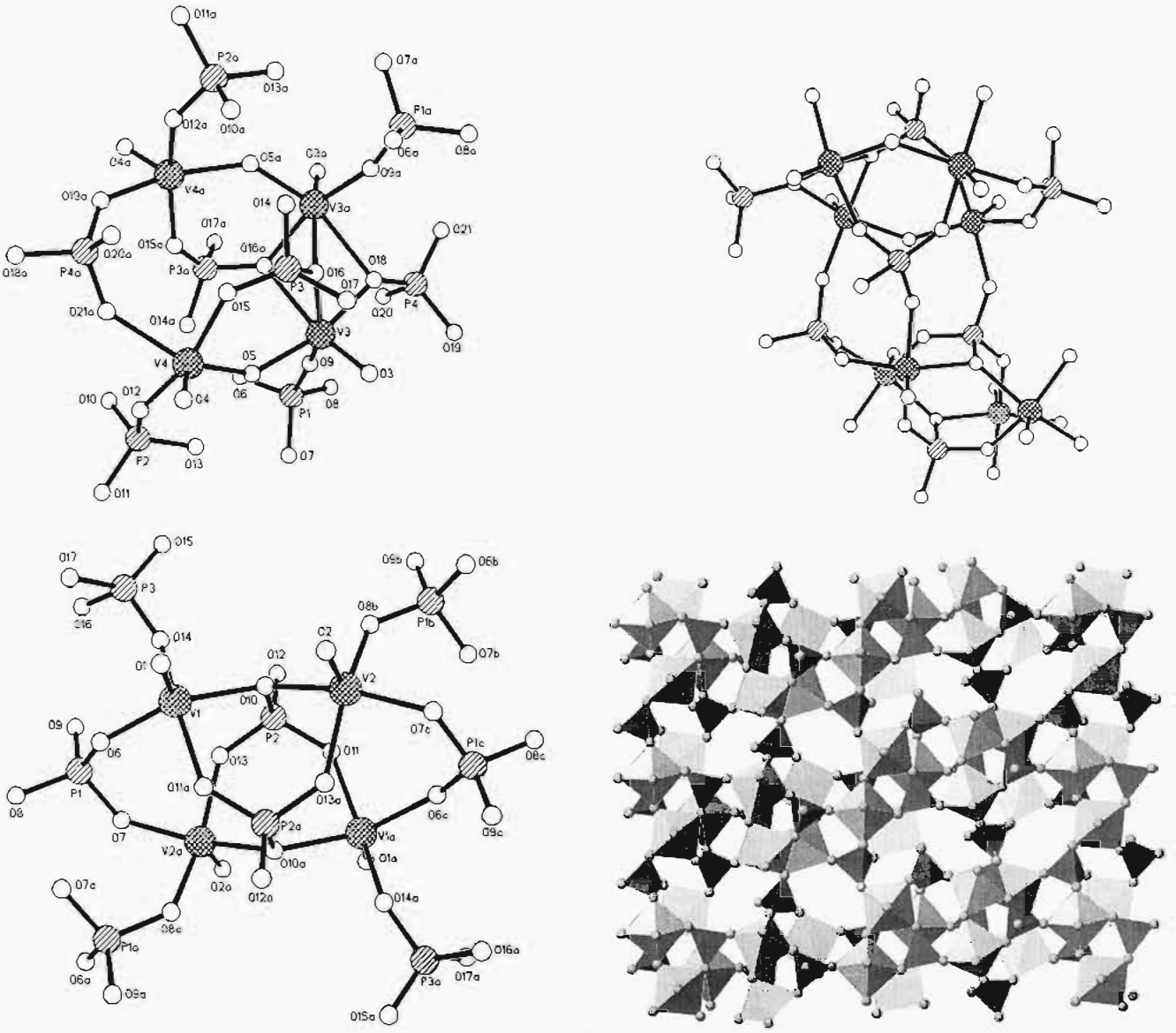

Figure 3. (a) Top left: View of the **3a** dimer of dimers motif of structure **3**, showing the atom-labeling scheme. (b) Bottom left: The second dimer of dimers unit **3b** with atom-labeling. (c) Top right: The linkage of **3a** and **3b** units. (d) Bottom right: Polyhedral view of the V−P−O layer of **3**.

The phosphate groups exhibit four distinct linkage modes. The P(1) sites serve as the "clips" linking the binuclear $\{V_2O_{10}\}$ halves of the **3b** fragments through O(6) and O(7), while the O(8) donor serves to bridge to an adjacent **3b** unit. The fourth oxygen O(9) of the P(1) phosphate bonds to a V(3) site of the **3a** tetranuclear unit. The P(2) phosphate site adopts the μ_4-bridging mode with respect to the **3b** unit, with O(10) bridging the V(1) and V(2) centers, while O(11) and O(13) adopt the symmetrically bridging bidentate mode with respect to the V(1a) and V(2a) sites of the same **3b** fragment. Phosphate unit P(3) employs O(16) to bridge V(3) and V(3a) of unit **3a**, while O(15) links to the V(4) site of the same **3a** cluster. Oxygen O(14) of the P(3) site serves to bridge to the V(1) center of an adjacent **3b** cluster, and since O(17) is protonated and pendant, the P(3) phosphate group is present as a $\{HPO_4\}^{2-}$ unit. Phosphate site P(4) participates exclusively in coordination to **3a** units. Oxygen atoms O(19) and O(21) bridge V(4) and V(4a) centers of a single **3a** moiety, while O(18) bridges V(3) and V(3a) sites of an adjacent **3a** group. The O(20) site is protonated, defining the P(4) phosphate group as a $\{HPO_4\}^{2-}$ unit. It is noteworthy that the P(3)−O(17) and P(4)−O(20) bond distances are 1.62(1) and 1.60(1) Å, respectively, compared to an average value of 1.52 Å for the remaining P−O bond lengths, clearly establishing these as the protonation sites.

As shown in Figure 3c, the **3a** units are linked through P(4) hydrogen phosphate tetrahedra into infinite ribbons. Similarly, infinite chains of **3b** sites linked by P(1) phosphate tetrahedra are constructed so as to run parallel to the **3a**-type chains and linked together via oxygen donors from P(1), P(2), and P(3) phosphate groups. This results in a layer constructed from alternating ribbons of **3a** and **3b** motifs linked via phosphate tetrahedra, as shown in Figure 3d.

Whereas the V/P/O layers of **1**−**3** are constructed from well-defined mononuclear, binuclear, and dimer of dimers motifs, the structure of **4** exhibits infinite chains of {V−O(H)−V} linked vanadium octahedra. The fundamental motif is the trinuclear unit described in Figure 4a, consisting of **face-sharing** $\{VO_6\}$ octahedra linked by corner sharing to a $\{VO_5\}$ square pyramid. Vanadium sites V(1) and V(2) exhibit distorted octahedral geometry, defined by three oxygen donors from each of three phosphate groups, which provides the common face, and, in the case of V(1), a terminal oxo group, a bridging

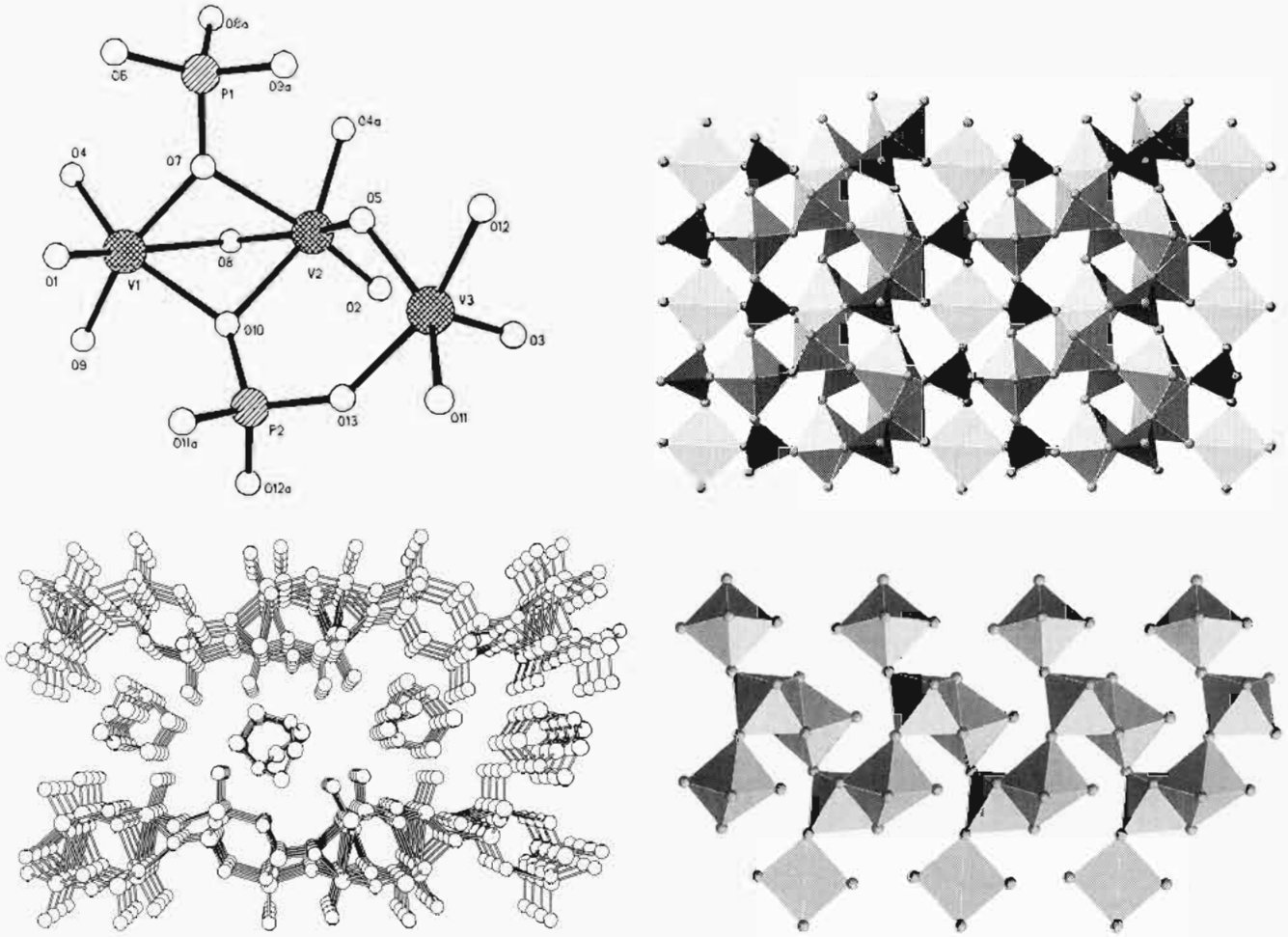

Figure 4. (a) Top left: Fundamental structural motif of the V−P−O layer of **4**. (b) Bottom left: View of the alternating inorganic/organic cation layers of **4**. (c) Top right: Polyhedral view of the V−P−O layer of **4**. (d) Bottom Right: Polyhedral representation of one of the one-dimensional chains which provide the backbone of the V−P−O layer structure of **4**.

hydroxy group, and the oxygen donor of a fourth phosphate ligand, while V(2) exhibits the ubiquitous terminal oxo group and two bridging hydroxy groups. The average V−O(4) and V−O(5) distance of 1.94 Å establishes these oxygen sites as hydroxy groups. However, in contrast to the generally symmetrical bridging modes adopted in **1**−**3** and for O(5) in **4**, the O(4) site of **4** exhibits a long−short bridging pattern with V(1)−O(4) of 1.98(7) Å and V(2)−O(4) of 1.869(7) Å. In this fashion, the binuclear units of face-sharing V(1)/V(2) octahedra are in turn connected through the O(4) hydroxy groups in corner-sharing linkages to produce an infinite chain of $\{VO_6\}$ octahedra with alternating corner-sharing and face-sharing connectivities. As shown in Figure 4d, the resultant undulating and kinked chain of $\{VO_6\}$ octahedra is fused at each V(2) site to a "pendant" V(3) square pyramid. These ribbons of vanadium octahedra and square pyramids are linked through the P(2) phosphate tetrahedra into the pattern of the V/P/O layer. As shown in Figure 4c, the P(2) phosphate site slots into the gaps formed between V(3) sites of adjacent ribbons of vanadium polyhedra.

It is noteworthy that while O(6) of phosphate P(1) does not coordinate to a vanadium site, it is not present as the pendant protonated {P−OH} moiety but rather as a {P=O} group, which appears to be strongly hydrogen-bonded to the $(H_2DABCO)^{2+}$ cations which are located in the interlamellar regions (Figure 4b). This feature is quite clear from the P(1)−O(6) bond distance of 1.50(6) Å, compared to an average P−O distance of 1.538 Å for all other phosphate oxygens of **4** and to a value of 1.61 Å for {P−OH} distances in **3**.

Conclusions

Hydrothermal synthesis may be exploited as a routine preparative technique for the isolation of complex, metastable inorganic materials from simple precursors. While the mechanisms of templating effects are not well understood, the manipulation of the hydrothermal reaction conditions permits the incorporation of different organic templates into the solid phase to produce two-dimensional V−P−O materials constructed of alternating inorganic and organic layers. The structural diversity and compositional range exhibited by **1**−**3** clearly reflect the profound influence of the template in directing the organization of the V−P−O layers. On the other hand, the characterization of two distinct layer structures with the same template for compounds **3** and **4** serves to emphasize the enigmatic nature of the template effect and the primitive evolution of rational control in these syntheses.

Compounds **1**−**4** reveal the unusual structural complexity which is possible from the linkage of simple inorganic precursors, in this case phosphate tetrahedra and vanadyl polyhedra. This structural diversity reflects the variability of vanadium coordination numbers, as well as the diverse connectivity patterns which may be generated between a given vanadium polyhedral type and the various phosphate tetrahedra $\{H_nPO_4\}^{(3-n)-}$ which may be present. Furthermore, the vanadium polyhedra may link to form clusters of various nuclearities which may in turn link through phosphate tetrahedra into complex networks. Further structural expansion is introduced by linking several vanadium-containing motifs into the structural

network. Thus, compound **1** contains only binuclear sites constructed of edge-sharing vanadium square pyramids, but **2** exhibits two distinct binuclear sites and a mononuclear site, all exhibiting square pyramidal geometry. Compound **3** not only contains two distinctive tetranuclear sites but features face-sharing vanadium octahedra as a component of one of these units. Finally, compound **4** possesses a layer structure constructed of infinite ribbons of corner- and face-sharing vanadium octahedra. Since the molecular chemistry of the oxovanadium core is characterized by species ranging from mononuclear to 34 vanadium superclusters, the question of what nuclearities may be incorporated into solid phases naturally arises. While mononuclear vanadium sites and binuclear up to pentanuclear clusters have been observed for V−P−O solid phases, large motifs, intermediate between the pentanuclear and the infinite chain, have yet to be encountered. Does this observation reflect a limitation on the V:P ratios for such solid phases? The upper limit for this study is V:P = 2.0; however, for most phases described to date the V:P ratio is generally close to 1.0, with many examples as low as 0.5. This reflects a requirement of reasonably high phosphate content to generate a negatively charged V−P−O network, which is characteristic of phases with lamellar or other open framework generated by incorporation of organic cations or templates.

Acknowledgment. The work at Syracuse University was funded by NSF Grant No. CHE9318824.

Supplementary Material Available: Tables of crystal data and experimental conditions, atomic positional parameters and isotropic temperature factors, bond lengths, bond angles, and anisotropic temperature factors for **1**−**4** (38 pages). Ordering information is given on any current masthead page.

IC9413833